Available online at www.sciencedirect.com
SCIENCE DIRECT®
Journal of Magnetic Resonance 167 (2004) 68–74
JMR Journal of Magnetic Resonance
www.elsevier.com/locate/jmr

Reducing the duration of broadband excitation pulses using optimal control with limited RF amplitude

Thomas E. Skinner,[a] Timo O. Reiss,[b] Burkhard Luy,[b] Navin Khaneja,[c] and Steffen J. Glaser[b,*]

[a] *Department of Physics, Wright State University, Dayton, OH 45435, USA*
[b] *Institut für Organische Chemie und Biochemie II, Technische Universität München, Lichtenbergstr. 4, 85747 Garching, Germany*
[c] *Division of Engineering and Applied Sciences, Harvard University, 29 Oxford Street, Cambridge, MA 02138, USA*

Received 18 September 2003; revised 1 December 2003

Abstract

Combining optimal control theory with a new RF limiting step produces pulses with significantly reduced duration and improved performance for a given maximum RF amplitude compared to previous broadband excitation by optimized pulses (BEBOP). The resulting pulses tolerate variations in RF homogeneity relevant for standard high-resolution NMR probes. Design criteria were transformation of $I_z \rightarrow I_x$ over resonance offsets of ± 20 kHz and RF variability of $\pm 5\%$, with a pulse length of 500 μs and peak RF amplitude equal to 17.5 kHz. Simulations transform I_z to greater than 0.995 I_x, with phase deviations of the final magnetization less than 2°, over ranges of resonance offset and RF variability that exceed the design targets. Experimental performance of the pulse is in excellent agreement with the simulations. Performance tradeoffs for yet shorter pulses or pulses with decreased digitization are also investigated.

Keywords: Broadband excitation; BEBOP; Optimal control theory

1. Introduction

Higher spectrometer field strengths provide significantly increased sensitivity and spectral resolution, but the sample must also be excited over a correspondingly expanded range of chemical shift frequencies. Ideally, one would like the excitation profile over the range to be uniform, producing transverse magnetization of constant phase. Considerable research effort has been devoted to developing such pulses [1–13]. However, keeping pace with steadily increasing field strength is a challenge, given maximum power tolerances for typical RF probes. Moreover, the focus in broadband excitation has primarily been on increasing the bandwidth of an ideally executed RF waveform. Dual compensation for RF inhomogeneity/miscalibration and chemical shift variation, with minimal J-modulation and relaxation during the pulse, are also desirable characteristics of a versatile broadband excitation pulse. Including these additional constraints on pulse performance makes the aforementioned challenge even more difficult.

Numerical optimization has always been an attractive option in principle, but the number of parameters required to define the problem can render classic optimization procedures (such as those in [14]) too computationally intensive to be practical. The combined number of RF parameters and resonance offsets multiplied by the total number of time increments can easily be on the order of thousands or more, increasing further if tolerance to RF inhomogeneity is included.

Optimal control theory [15–18] is a well-known and widely used technique that provides an enormous efficiency gain compared to traditional procedures. Its use in optimizing fuel efficiency for the Apollo Mission to the moon is an often cited example of its utility. Other examples include robot control and satellite guidance, as

* Corresponding author.
E-mail address: glaser@ch.tum.de (S.J. Glaser).

1090-7807/$ - see front matter © 2003 Elsevier Inc. All rights reserved.
doi:10.1016/j.jmr.2003.12.001

noted in [19]. Our initial attempt using this method produced a 2 ms pulse (peak RF amplitude 17.5 kHz) which is insensitive to J-coupling effects and excites transverse magnetization of nearly constant phase over resonance offsets of 40 kHz with up to 4 dB tolerance to RF miscalibration [20]. Prior to this, optimal control in NMR appears to have been confined to narrowband selective excitation for magnetic resonance imaging applications [19,21,22].

We report further improvements in broadband excitation by optimized pulses (BEBOP), employing the basic excitation pulse to develop optimal control algorithms that will subsequently find use in other NMR applications. Although the 2 ms BEBOP performs extremely well, shorter pulses are also desirable in order to minimize relaxation effects. At the same time, peak RF amplitude must remain below probe limits (e.g., available for ^{13}C spectroscopy). In our previous algorithm for implementing the theory, the maximum amplitude of the RF controls was constrained indirectly—a chosen pulse length and convergence factor for terminating the algorithm resulted in an unspecified maximum pulse amplitude. We now clip the RF amplitude at the previous 17.5 kHz peak value and force the optimal control algorithm to search for another solution whenever the amplitude exceeds this limit. The utility of the new approach is demonstrated by the design of a 500 μs BEBOP with performance characteristics that surpass the 2 ms pulse. Alternatively, performance matching the 2 ms pulse is attainable by designing either a shorter pulse (400 μs) or a separate 500 μs BEBOP derived using significantly decreased digitization.

2. Theory and methods

The following brief overview of optimal control theory, as it relates to excitation in NMR, provides a basis for defining the BEBOP numerical algorithm. Further details can be found in [20].

2.1. Optimal control theory: application to excitation

The broadband excitation problem defines a standard constrained optimization: during the time interval $[t_0, t_p]$, transfer initial magnetization $\boldsymbol{M}(t_0) = \hat{\boldsymbol{z}}$ to the target final state $\boldsymbol{F} = \hat{\boldsymbol{x}}$ for a specified range of chemical-shift offsets and a desired degree of tolerance to RF inhomogeneity or miscalibration. The trajectories $\boldsymbol{M}(t)$ are constrained by the Bloch equation

$$\dot{\boldsymbol{M}} = \boldsymbol{\omega}_e \times \boldsymbol{M}. \tag{1}$$

We write the effective RF field $\boldsymbol{\omega}_e$ in angular frequency units (radians/s) in the rotating frame as

$$\boldsymbol{\omega}_e = \omega_1(t)[\cos\phi(t)\ \hat{\boldsymbol{x}} + \sin\phi(t)\ \hat{\boldsymbol{y}}] + \Delta\omega(t)\ \hat{\boldsymbol{z}}, \tag{2}$$

which encompasses any desired modulation of the amplitude ω_1, phase ϕ, and frequency offset $\Delta\omega$ of the pulse.

Constraints on the optimization can be effectively incorporated into the formalism using the technique of Lagrange multipliers (for example [23]). The vector Bloch equation thus introduces a vector Lagrange multiplier $\boldsymbol{\lambda}$. We seek to optimize a final cost function

$$\Phi = \boldsymbol{M}(t_p) \cdot \boldsymbol{F}, \tag{3}$$

which quantifies the degree to which $\boldsymbol{M}(t_p) = \boldsymbol{F}$. Then, the necessary conditions that must be satisfied at each time for the cost given in Eq. (3) to be maximized are:

$$\dot{\boldsymbol{M}} = \boldsymbol{\omega}_e \times \boldsymbol{M}, \quad \boldsymbol{M}(t_0) = \hat{\boldsymbol{z}}, \tag{4}$$

$$\dot{\boldsymbol{\lambda}} = \boldsymbol{\omega}_e \times \boldsymbol{\lambda}, \quad \boldsymbol{\lambda}(t_p) = \boldsymbol{F}, \tag{5}$$

$$\boldsymbol{M} \times \boldsymbol{\lambda} = 0. \tag{6}$$

Thus, both $\boldsymbol{M}$ and $\boldsymbol{\lambda}$ obey the Bloch equation. As noted previously [20], a sequence which transforms $\boldsymbol{M}(t_0)$ forward in time to the desired target state $\boldsymbol{F}$ therefore transforms $\boldsymbol{\lambda}(t_p) = \boldsymbol{F}$ backwards in time to $\boldsymbol{M}(t_0)$. Since $\boldsymbol{\omega}_e(t)$ controls the evolution of $\boldsymbol{M}(t)$, the goal of finding the optimum trajectory is the same as finding the optimal RF sequence to apply to the sample. For the optimal pulse, we then have $\boldsymbol{M}_{opt}(t) = \boldsymbol{\lambda}_{opt}(t)$, which satisfies the stationary condition given by Eq. (6). For a non-optimal pulse, $\boldsymbol{M} \times \boldsymbol{\lambda}$ at each time point of the two trajectories gives the proportional adjustment to make in the control field $\boldsymbol{\omega}_e(t)$.

2.2. Numerical algorithm

The procedure for optimizing the cost, subject to the constraint that the RF amplitude at each time, $\omega_1(t)$, be no greater than a chosen maximum amplitude ω_{max}, is incorporated in the following algorithm:

(i) Choose an initial RF sequence $\boldsymbol{\omega}_e^{(0)}$.
(ii) Evolve $\boldsymbol{M}$ forward in time from the initial state $\hat{\boldsymbol{z}}$.
(iii) Calculate $\boldsymbol{M}(t_p) \times \boldsymbol{\lambda}(t_p)$ and evolve it backwards in time.
(iv) $\boldsymbol{\omega}_e^{(k+1)}(t) \rightarrow \boldsymbol{\omega}_e^{(k)}(t) + \epsilon[\boldsymbol{M}(t) \times \boldsymbol{\lambda}(t)]$.
(v) For any $\omega_1(t) > \omega_{max}$, set $\omega_1(t) \rightarrow \omega_{max}$.
(vi) Repeat steps (ii)–(v) until a desired convergence of Φ is reached.

The RF clipping in step (v) is implemented by adjusting $(\omega_1)_x$ and $(\omega_1)_y$ to satisfy the constraint on maximum RF amplitude without changing the phase of ω_1. Additional details concerning each step and adjustments related to the demands of broadband excitation are described next.

2.3. Broadband excitation

For broadband excitation, the ideal cost, $\boldsymbol{M}_x(t_p) = 1$, which is necessary to satisfy Eq. (6) and terminate the

algorithm, cannot be achieved by an optimal sequence at all resonance offsets simultaneously. For a range of chemical shift offsets, and also a range of nonideal RF fields, the average cost $\langle \boldsymbol{M}_x(t_p)\rangle < 1$. Therefore, the value of $\boldsymbol{M} \times \boldsymbol{\lambda}$ is calculated for each combination of resonance offset and RF field, and the average of all these values, $\langle \boldsymbol{M} \times \boldsymbol{\lambda}\rangle$, is used in step (iii), since it can converge to zero and terminate the algorithm.

Since typical spectrometers implement frequency modulation as a phase modulation, with $\Delta\omega(t) = \mathrm{d}\phi(t)/\mathrm{d}t$, only amplitude and phase modulation were used in the algorithm. Thus, only the transverse or (x, y) components of $\boldsymbol{\omega}_e$ are modified in step (iv). The value of $\Delta\omega$ in Eq. (2) is time-independent, and gives the chemical shift of the irradiated spin. A sequence of random (x, y) amplitudes was generated to initiate the algorithm in step (i). The two RF control fields $(\boldsymbol{\omega}_1)_x$ and $(\boldsymbol{\omega}_1)_y$ were digitized in 0.5 μs steps over the 500 μs pulse length. The same digitization was used in deriving a shorter 400 μs pulse, and an additional 500 μs pulse was derived using a 5 μs digitization. RF inhomogeneity in the amplitude $\omega_1(t)$ was incorporated by scaling the ideal RF amplitude $\omega_1^0(t)$ according to $\omega_1(t) = \alpha\omega_1^0(t)$ for constant factors α.

Using steps (ii) and (iii), the average $\langle \boldsymbol{M} \times \boldsymbol{\lambda}\rangle$ was calculated over a combination of 41 resonance offsets in the range ±20 kHz, incremented by 1000 Hz, and five RF scalings given by $\alpha = (0.95, 0.975, 1.0, 1.025, 1.05)$. The RF values were weighted according to a Gaussian distribution $\exp[-(1-\alpha)^2/(2\sigma^2)]$, with $\sigma = 0.042$ giving a full width at half-maximum (FWHM) of 0.1, or 10% of the nominal RF value. The resonance offsets were weighted equally.

In step (iv), the RF is incremented by the largest value of ϵ that provides improvement in the cost, determined at each iteration by bracketing the optimal step size among three values and using a simple 1D line minimization routine [14]. The efficiency of the optimization was further enhanced using a conjugate gradient method to determine the step direction.

3. Results and discussion

Previously [20], RF power was limited indirectly in the optimal control procedure. The pulse length and convergence parameter for terminating the algorithm were set sufficiently large that acceptable performance was obtained without exceeding the power limits of typical ^{13}C probes. We obtained a 2 ms pulse with maximum RF amplitude equal to 17.5 kHz capable of transforming 99.5% of initial z magnetization to within 4° of the x axis over resonance offsets of ±20 kHz and a variation of ±5% in the optimal RF calibration. By implementing the new clipping algorithm, we have been able to further improve pulse performance for the same maximum RF amplitude, while reducing the pulse length by a factor of 4. The amplitude and phase of the resulting excitation pulse, digitized in 0.5 μs increments, are plotted as a function of time in Fig. 1 for comparison with the earlier result. The figure clearly shows the cutoff for the maximum RF amplitude, resulting in a constant amplitude of 17.5 kHz during extended periods of the pulse. The inverse transformation $I_x \rightarrow I_z$ can be obtained by applying the time-reversed pulse, with each phase incremented by 180°.

The theoretical performance of the pulse, assuming simple Bloch equation evolution of the irradiated spins (as in the optimization procedure), is illustrated in Fig. 2. Contours of x magnetization, M_x, are plotted in the upper panel as functions of resonance offset and RF inhomogeneity. The phase of the excited magnetization is shown similarly in the lower panel. Over a ±5% variation in the nominal RF delivered by the coil and resonance offsets of ±20 kHz, the excited magnetization M_x is still at least 99.5% of the initial z magnetization, M_0, but the phase is now less than 2°, compared to 4° for the 2 ms pulse. The 99% contours cover almost a ±15% variation in nominal RF, and the phase of the final magnetization is on the order of only 4° over this larger RF range, operating over the same 40 kHz bandwidth.

The rapid and sometimes large changes in RF amplitude of the pulse might be expected to place rather high demands on the output fidelity of system hardware. To date, we have found BEBOP demands no more than is required of any shaped pulse—namely, that RF output

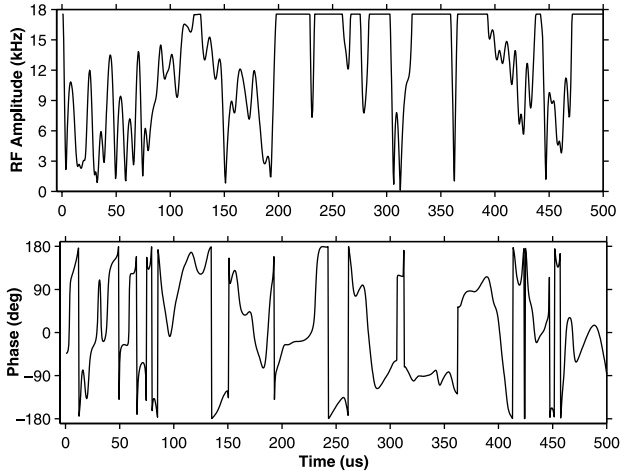

Fig. 1. Broadband excitation pulse obtained using the optimal control algorithm described in the text. Application of pulse amplitude (upper panel) and phase (lower panel) produces the transformation $I_z \rightarrow I_x$ over a 40 kHz range of resonance offsets with tolerance to RF miscalibration sufficient for typical high-resolution NMR probes (see Fig. 2). The maximum RF amplitude was limited to 17.5 kHz by clipping whenever the amplitude exceeded this value, forcing the algorithm to search for another solution. A 500 μs pulse of constant 13.5 kHz RF amplitude would have the same power requirements as the pulse shown.

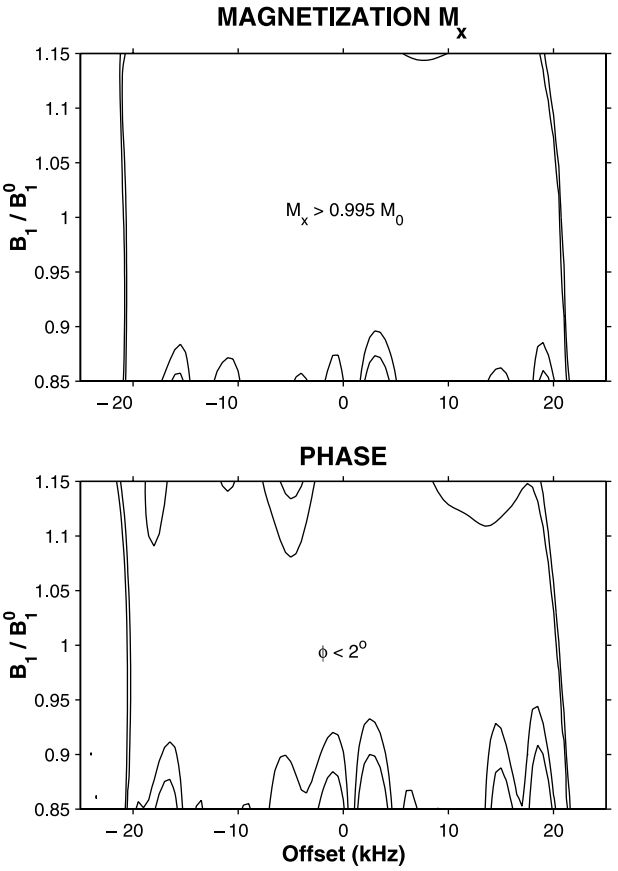

Fig. 2. Simulated performance of the optimized pulse of Fig. 1. Starting with initial z magnetization M_0, the magnitude M_x (upper panel) and phase ϕ (lower panel) of the excited magnetization are plotted as a function of resonance offset and RF field B_1, represented as a fraction of the nominal field B_1^0. Contour lines displayed for M_x are [0.995, 0.99], and those for the phase of the excited magnetization are [2°, 4°], demonstrating practically ideal performance even beyond the range of RF (±5%) and resonance offset (±20 kHz) variations considered in the optimal control implementation.

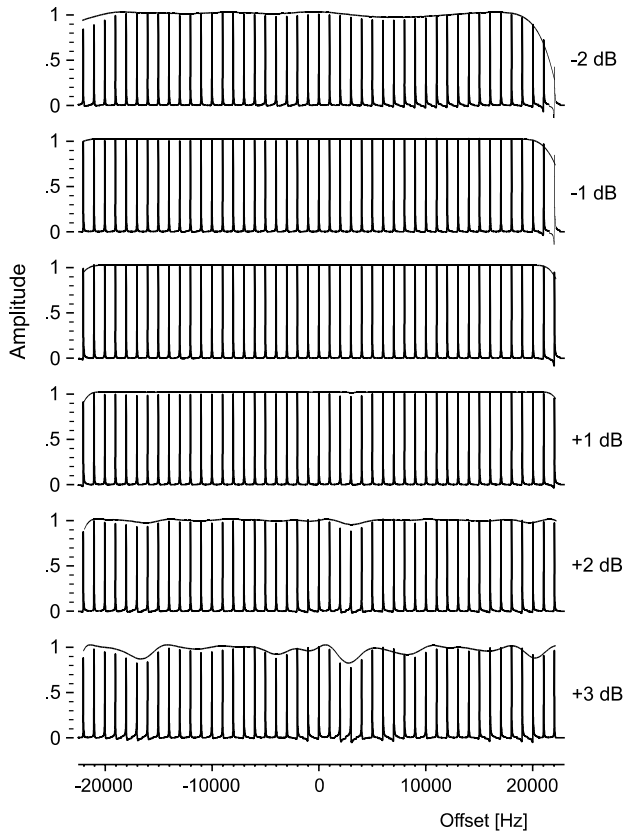

Fig. 3. Excitation profiles for the residual HDO signal in a sample of 99.96% D_2O are displayed as a function of resonance offset and RF power levels applied to the sample using the 500 μs pulse of Fig. 1. Power levels were varied in 1 dB increments by adjusting attenuation relative to the calibrated pulse at 0 dB, resulting in peak RF amplitudes of 22 kHz (−2 dB), 19.6 kHz (−1 dB), 17.5 kHz (0 dB), 15.6 kHz (+1 dB), 13.9 kHz (+2 dB), and 12.4 kHz (+3 dB). The solid line at the top of each set of profiles is the theoretical performance of the pulse, plotted, as in Fig. 2, as the value of M_x after excitation of initial z magnetization, M_0. The experimental performance of the pulse is excellent, producing almost perfect excitation, $M_x > 0.995\ M_0$, over ±20 kHz for RF variability within 1 dB (±12%) of the calibrated value, which exceeds the ±5% variation targeted in the optimization.

be linear as a function of RF power. Deviations from linearity are effectively corrected in software. Details related to pulse implementation on our particular system are provided in Section 4.

As shown in Fig. 3, the experimental performance of the pulse is in excellent agreement with the simulations. The calibrated pulse at 0 dB (17.5 kHz peak RF) and pulses applied with attenuations of ±1 dB (−12.6%, +12.0%) relative to the calibrated RF values match the nearly ideal performance shown in the simulations. At ±2 dB (−20.6%, +25.9%), the pulse still provides tolerable performance, with $M_x > 0.95$ at most resonance offsets in the 40 kHz range, and M_x slightly less then 0.9 at a few offsets. Pulse performance is finally significantly degraded at a +3 dB (−29.3%) reduction in the calibrated values. Nonetheless, the performance of the pulse is quite good outside the ±5% (∼±0.4 dB) range of RF inhomogeneity it was designed to accommodate.

Previously [20], as a benchmark for pulse performance, we considered a transverse magnetization equal to at least 95% of the initial equilibrium value, with a phase roll of no more than 4° over the resonance offset range. For the new 500 μs BEBOP, a figure-of-merit (FOM), defined as the total excitation bandwidth satisfying the benchmark divided by the peak RF amplitude, is in the range 2.3–2.4 for B_1/B_1^0 in the range 0.9–1.15. This represents a considerable improvement over the RF compensation of a phase-corrected hard pulse, which only provides a slightly higher FOM = 2.5 for the ideal calibrated value, $B_1/B_1^0 = 1$. For further comparison purposes, as noted in [20], a hard 90° pulse of amplitude 17.5 kHz, after phase correction of the spectrum, gives $M_x > 0.995\ M_0$ over offsets of only ±12 kHz for the calibrated value and ±6 kHz for RF variability $0.95 \leqslant B_1/B_1^0 \leqslant 1.05$.

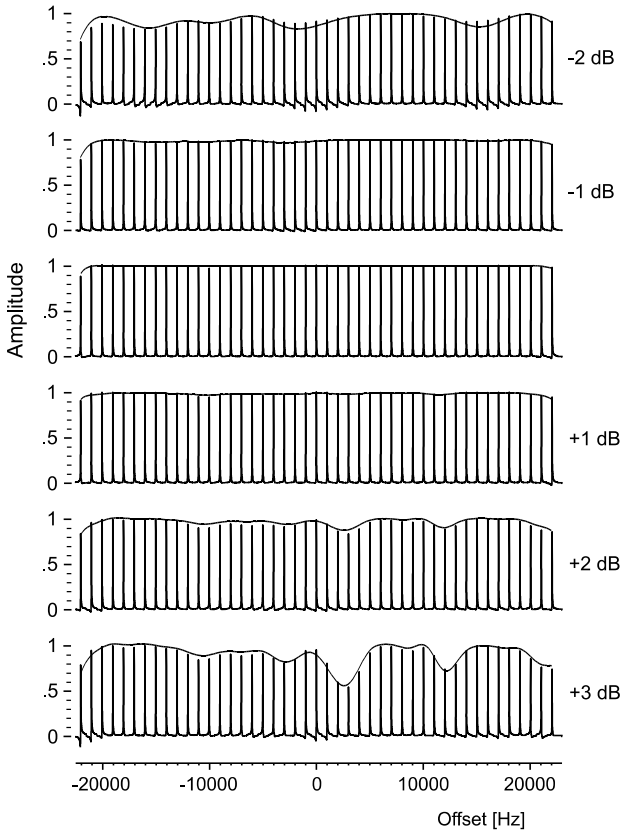

Fig. 4. Excitation profiles for a 400 μs pulse derived using the same design criteria as for the 500 μs pulse demonstrated in Fig. 3.

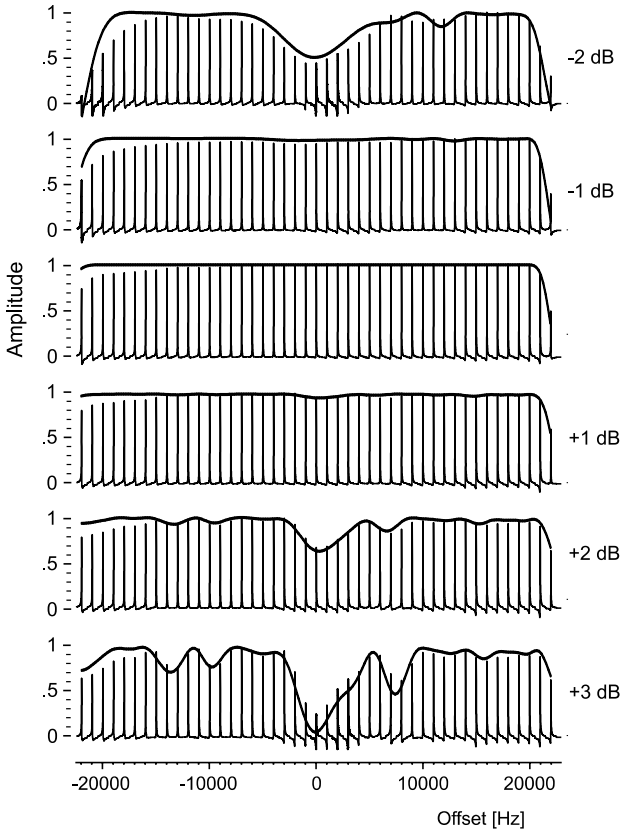

Fig. 5. Excitation profiles for a 500 μs pulse derived using the same design criteria as for the 500 μs pulse demonstrated in Fig. 3, except the digitization of this pulse has been reduced by a factor of 10.

The best of previous broadband excitation pulses [6,10] demand less of system hardware, but provide performance comparable to BEBOP only at the ideal RF values. The ABSTRUSE pulse [13] actually provides a greater excitation bandwidth for a given peak RF amplitude than any of the other pulses cited, but it is 12 ms long and highly vulnerable to J-coupling and relaxation effects. More importantly, all the excitation pulses cited [1–13] exhibit a significant drop in performance when the effects of RF inhomogeneity are included. If no RF compensation is required, optimal control without the new clipping algorithm has already provided a 2 ms pulse with nearly perfect excitation, $M_z \rightarrow 0.999\,M_x$, over a bandwidth of 100 kHz, requiring only a modest 10% increase in the original 17.5 kHz peak amplitude [20]. This represents a dramatic increase in excitation bandwidth compared to any previous excitation strategies. However, the impact of such a pulse will be less pronounced without dual compensation for RF and chemical shift variation. Nonetheless, it indicates there is considerable scope for improving pulse performance without increasing peak power.

The nearly ideal pulse performance illustrated in Fig. 2 indicates that there is some latitude within the constraints of the design criteria for further shortening the pulse length, since perfect performance may not be necessary. Alternatively, we can consider keeping the pulse length the same and decrease the digitization of the pulse in the optimal control algorithm to reduce demands on hardware for rapid shifting of amplitude and phase. Two additional pulses were derived, accordingly.

The experimental performance of a 400 μs pulse designed using the same 0.5 μs digitization as the first pulse is shown in Fig. 4. Although the range of tolerance to RF inhomogeneity is reduced compared to the original 500 μs pulse, this shorter pulse still performs exceptionally well within 1 dB of the calibrated RF amplitude, which exceeds the design limits given in the optimal control algorithm.

Similarly, the performance of a 500 μs pulse digitized in 5 μs increments is shown in Fig. 5. Although the performance of these two alternative pulses is not as ideal as the pulse of Fig. 1, contour plots as in Fig. 2 match the excellent performance of the original 2 ms BEBOP of [20].

4. Experimental

Experimental excitation profiles were implemented on a Bruker DMX 900 spectrometer equipped with modern

SGU units for RF control and linearized amplifiers. A sample of 99.96% D_2O was doped with $CuSO_4$ to a final T_1 relaxation time of ~500 ms. To reduce effects due to strong B_1-field inhomogeneity in the 900 MHz cryogenic probe that is installed on the system, approximately 40 μl of this solution was placed in a Shigemi limited volume tube.

The pulse requires accurate RF output from system hardware. However, we have not found the rapid changes in pulse amplitude noted earlier to be a problem for modern NMR consoles. Our initial implementation of the pulse using the generic system hardware and software produced quite good results that nonetheless failed to match theoretical expectations. We therefore monitored the experimentally produced pulse shape and found an *inverse* droop of 4–8% (increase in RF output as a function of time) for our particular SGU/amplifier combination. Since the profile of the amplitude increase was most pronounced at the beginning of the pulse and flattened out near the end of the pulse, we used a simple workaround to avoid the observed amplitude enhancement. The length of the pulse was increased by adding a period of zero amplitude at the beginning, where the most serious corruption of the pulse shape occurs. Adding a delay of three times the pulse length to the shape reduced the initial inverse droop in the experimentally obtained pulse shape to a relatively small 1% increase in the amplitude.

The maximum RF amplitude was calibrated using a square shaped pulse, again initially zero-filled. Offset profiles were then obtained for the 500 and 400 μs broadband excitation by varying the offset of the shaped pulses from −22,000 to 22,000 Hz in steps of 1000 Hz. In order to also monitor the B_1-field dependence of the pulses the experiments were repeated with ±1, ±2, and +3 dB attenuation relative to the calibrated RF amplitude, corresponding to maximum RF fields of 12,380, 13,900, 15,600, 17,500, 19,620, and 22,030 Hz. The results are shown in Fig. 3 (500 μs pulse), Fig. 4 (400 μs pulse), and Fig. 5 (separate 500 μs pulse with only 100 time steps) with the theoretical magnitude of M_x after excitation drawn on top of the individual offset profiles. The experimental data match theory almost perfectly for the 500 and 400 μs pulses. Only the 500 μs pulse derived with reduced digitization displays slight deviations, especially at high-frequency offsets. In this case, the differences between simulation and experiment are likely due to the implementation of the offset profiles, since the offset was realized by a linear phase ramp added to the shaped pulse. For the 100-point 500 μs pulse, the resulting phase increment of 36° per time step is relatively large, and the corresponding digitization artifacts are not negligible compared to the 1000-point pulses.

5. Conclusion

A 500 μs implementation of BEBOP has been demonstrated. The pulse, digitized in 0.5 μs increments, has a peak RF amplitude of 17.5 kHz and is tolerant to a range of RF inhomogeneity (±2 dB) that is more than sufficient for high-resolution NMR probes. It produces final magnetization of essentially uniform phase over resonance offsets of 40 kHz. BEBOP was designed by adding a simple RF limiting step to our previous optimal control procedure [20], enabling the algorithm to find a nearly ideal solution with a fourfold reduction in pulse length for the same peak RF. Using the same design criteria as for the first pulse, we also derived a 400 μs BEBOP, as well as a 500 μs pulse with significantly reduced digitization (5 μs per RF increment). Both of these additional pulses exhibit quite good experimental performance.

Even shorter pulses may be possible. We plan to consider the effect of other expressions for the final cost Φ and also investigate the limits of tolerance to RF inhomogeneity. We will continue to develop algorithms using excitation as a particularly simple example that allows a clear delineation between the effects of optimal control and the application, which might be less apparent with a more complicated sequence. BEBOP pulses obtained to date can be downloaded in Bruker and Varian formats from http://www.org.chemie.tu-muenchen.de/people/bulu/.

Acknowledgments

B.L. thanks the Fonds der Chemischen Industrie and the Deutsche Forschungsgemeinschaft (Emmy Noether fellowship LU 835/1-1) for support. S.J.G. acknowledges support from the Deutsche Forschungsgemeinschaft for Grants Gl 203/3-1 and Gl 203/4-1 and the Fonds der Chemischen Industrie. N.K. would like to acknowledge Darpa Grant F49620-0101-00556.

References

[1] R. Freeman, S.P. Kempsell, M.H. Levitt, Radiofrequency pulse sequences which compensate their own imperfections, J. Magn. Reson. 38 (1980) 453–479.
[2] M.H. Levitt, Symmetrical composite pulse sequences for NMR population inversion. I. Compensation of radiofrequency field inhomogeneity, J. Magn. Reson. 48 (1982) 234–264.
[3] M.H. Levitt, R.R. Ernst, Composite pulses constructed by a recursive expansion procedure, J. Magn. Reson. 55 (1983) 247–254.
[4] R. Tycko, H.M. Cho, E. Schneider, A. Pines, Composite pulses without phase distortion, J. Magn. Reson. 61 (1985) 90–101.
[5] M.H. Levitt, Composite pulses, Prog. Nucl. Magn. Reson. Spectrosc. 18 (1986) 61–122.

[6] A.J. Shaka, A.J. Pines, Symmetric phase-alternating composite pulses, J. Magn. Reson. 71 (1987) 495–503.
[7] J.-M. Böhlen, M. Rey, G. Bodenhausen, Refocusing with chirped pulses for broadband excitation without phase dispersion, J. Magn. Reson. 84 (1989) 191–197.
[8] J.-M. Böhlen, G. Bodenhausen, Experimental aspects of chirp NMR spectroscopy, J. Magn. Reson. Ser. A 102 (1993) 293–301.
[9] D. Abramovich, S. Vega, Derivation of broadband and narrow-band excitation pulses using the Floquet Formalism, J. Magn. Reson. Ser. A 105 (1993) 30–48.
[10] Ē. Kupče, R. Freeman, Wideband excitation with polychromatic pulses, J. Magn. Reson. Ser. A 108 (1994) 268–273.
[11] K. Hallenga, G.M. Lippens, A constant-time ^{13}C–^{1}H HSQC with uniform excitation over the complete ^{13}C chemical shift range, J. Biomol. NMR 5 (1995) 59–66.
[12] T.-L. Hwang, P.C.M. van Zijl, M. Garwood, Broadband adiabatic refocusing without phase distortion, J. Magn. Reson. 124 (1997) 250–254.
[13] K.E. Cano, M.A. Smith, A.J. Shaka, Adjustable, broadband, selective excitation with uniform phase, J. Magn. Reson. 155 (2002) 131–139.
[14] W.H. Press, S.A. Teukolsky, W.T. Vetterling, B.P. Flannery, Numerical Recipes in C, Cambridge University Press, New York, NY, 1988.
[15] L. Pontryagin, B. Boltyanskii, R. Gamkrelidze, E. Mishchenko, The Mathematical Theory of Optimal Processes, Wiley-Interscience, New York, 1962.
[16] A.P. Sage, Optimum Systems Control, Prentice-Hall, Englewood Cliffs, NJ, 1968.
[17] A. Bryson Jr., Y.-C. Ho, Applied Optimal Control, Hemisphere, Washington, DC, 1975.
[18] E. Pinch, Optimal Control and the Calculus of Variations, Oxford University Press, Oxford, 1993.
[19] S. Conolly, D. Nishimura, A. Macovski, Optimal control solutions to the magnetic resonance selective excitation problem, IEEE Trans. Med. Imaging MI-5 (1986) 106–115.
[20] T.E. Skinner, T.O. Reiss, B. Luy, N. Khaneja, S.J. Glaser, Application of optimal control theory to the design of broadband excitation pulses for high resolution NMR, J. Magn. Reson. 163 (2003) 8–15.
[21] J. Mao, T.H. Mareci, K.N. Scott, E.R. Andrew, Selective inversion radiofrequency pulses by optimal control, J. Magn. Reson. 70 (1986) 310–318.
[22] D. Rosenfeld, Y. Zur, Design of adiabatic selective pulses using optimal control theory, Magn. Reson. Med. 36 (1996) 401–409.
[23] H. Goldstein, Classical Mechanics, Addison-Wesley, Reading, MA, 1980.